Diffusion limit of langevin pdf models in weakly inhomogeneous turbulence

Casimir Emako, Viviana Letizia, Nadia Petrova, Rémi Sainct, Roland Duclous, Olivier Soulard

ESAIM: PROCEEDINGS, Vol. ?, 2014, 1-10
Editors: Will be set by the publisher

DIFFUSION LIMIT OF LANGEVIN PDF MODELS IN WEAKLY INHOMOGENEOUS TURBULENCE*

C. Emako[1], V. Letizia[2], N. Petrova[3], R. Sainct[4], R.Duclous[5] et O. Soulard[5]

Résumé. Dans cet article, nous abordons la question de la modélisation du transport turbulent dans les modèles de turbulence basés sur les fonctions de densité de probabilité (PDF). Nous étudions la limite diffusive de ces modèles obtenue lorsque l'advection et la dissipation sont les seuls processus physiques actifs. Dans cette limite, nous montrons que les modèles PDF donnent lieu à un développement asymptotique selon un petit paramètre correspondant au rapport de l'échelle intégrale sur l'échelle du gradient moyen. La contribution principale de ce développement s'identifie avec un modèle $\overline{k} - \overline{\varepsilon}$ classique. En particulier, le transport de l'énergie turbulente est donné par une diffusion en premier gradient. L'identification entre modèle $\overline{k} - \overline{\varepsilon}$ et modèle PDF permet de soulever un certain nombre de questions sur la manière dont le transport est modélisé dans les approches PDF. La solution asymptotique est validée par des simulations numériques réalisées à l'aide d'un code Monte Carlo mais aussi d'un code déterministe.

Abstract. In this work, we discuss the modelling of transport in Langevin probability density function (PDF) models used to predict turbulent flows [1]. Our focus is on the diffusion limit of these models, i.e. when advection and dissipation are the only active physical processes. In this limit, we show that Langevin PDF models allow for an asymptotic expansion in terms of the ratio of the integral length to the mean gradient length. The main contribution of this expansion yields an evolution of the turbulent kinetic energy equivalent to that given by a $k - \varepsilon$ model. In particular, the transport of kinetic energy is given by a gradient diffusion term. Interestingly, the identification between PDF and $\overline{k} - \overline{\varepsilon}$ models raises a number of questions concerning the way turbulent transport is closed in PDF models. In order to validate the asymptotic solution, several numerical simulations are performed.

1. Introduction

Since the early work of Pope [1], the so-called probability density function (PDF) approach has proved to be an efficient tool for predicting turbulent flows. In this approach, one derives and solves a modeled transport equation for the one-point PDF of the fluctuating velocity field and, when necessary, of additional variables describing the state of the flow, such as concentration, temperature or density. In the modeling process of the flow one-point statistics, closures must be applied to the turbulent acceleration as well as to molecular diffusion

* *This work has been performed during the CEMRACS-2013 at Luminy. The authors would like to thank Nicolas Champagnat, Tony Lelievre and Anthony Nouy for the organization, and acknowledge the Labex AMIES for its support.*

[1] UPMC Univ Paris 06, UMR 7598, Laboratoire Jacques-Louis Lions, F-75005, Paris, France
[2] Univ Paris-Dauphine, UMR 7534, Laboratoire Ceremade, F-75016, Paris, France
[3] ONERA
[4] Ecole des Ponts ParisTech, Laboratoire Cermics
[5] CEA, DAM, DIF, F-91297, Arpajon, France

terms. Most of these closures yield a PDF transport equation of the Langevin type [1–4]. In this work, we will only focus on this class of models.

While mostly used to predict turbulent reactive flows, the PDF approach has also demonstrated its utility for solving incompressible inert flows. In this context, Langevin PDF models have been shown [2] to be connected to simpler turbulent models which focus solely on the second-order one-point correlation tensor of the velocity field, also called Reynolds stress tensor. These Reynolds stress models (RSM) revert to the well known $k-\varepsilon$ model when turbulence is isotropic. The PDF/RSM equivalence encompasses most physical processes at work in incompressible flows, including production, non-linear redistribution and dissipation effects. However, strong differences exist in the way both approaches deal with the transport of the turbulent kinetic energy and of its anisotropy.

In RSM, turbulent transport is usually modeled by a gradient diffusion assumption. Many variants of this closure exist, but most are found to yield similar results in practical situations [5, 6]. In the PDF approach, the situation is different. The advection term appearing in the Navier-Stokes equations does not require any closure. In that sense, turbulent advection is often said to be treated "exactly" or "without assumption" [4, 7]. However, such statements might be somewhat misleading. Indeed, the overall process of turbulent transport is not exact since the statistics of the velocity field are affected by the Langevin closures used in the remaining parts of the PDF transport equation.

Thus, turbulent transport and Langevin closures are interacting in PDF models. This interaction is flow-dependent and cannot be made explicit in the general case. Yet, when non-equilibrium/production effects become negligible, the PDF equation is expected to degenerate and to yield a gradient diffusion formulation for the transport of Reynolds stresses. This is suggested by several works, for instance [2, 5, 8], which focus on triple velocity correlations and on their expression in the absence of production. As a consequence, in this diffusion limit, a PDF/RSM equivalence should exist for the turbulent transport term. Then, significant knowledge could be gained by comparing the two families of models, just as it was done in the homogeneous case by Pope [2].

However, the diffusion limit of PDF models has never been looked at thoroughly. The precise conditions under which it occurs have not been explicited. Besides, the influence of dissipation processes are usually discarded while they are expected to play a significant role. Finally and more importantly, the study of the diffusion limit has been limited to considerations on the sole triple velocity correlations and not on the PDF itself.

Thus, the purpose of this work is to study the diffusion limit of PDF Langevin models and to explicit the connection with RSM models in that particular case. To this end, we consider a simplified setting in which diffusion and dissipation are the only active physical mechanisms. Then, we look for an asymptotic expansion of the Langevin PDF equation in terms of the ratio of the integral to the mean gradient length. The relevance of this expansion is verified on several simulations. Finally, its implications in terms of physical models are discussed.

2. Simplified Langevin PDF model applied to a turbulent zone

Throughout this work, we will consider a canonical turbulent flow consisting in a 1D slab of turbulence that decays and diffuses with time. This flow is sketched in figure 1 and will be refered to as turbulent zone (TZ). The inhomogeneous direction is denoted by x_1 and the length of the TZ by L_{TZ}. Our interest lies in finding the properties of the PDF $f(\mathbf{u}; x_1, t)$ of the velocity field $\mathbf{u} = (u_1, u_2, u_3)$ at point x_1 and time t when modelled by the simplified Langevin model (SLM) [1]. In the TZ configuration and with the SLM, the evolution of f is given by :

$$\frac{\partial f}{\partial t} + u_1 \frac{\partial f}{\partial x_1} = -\frac{\partial}{\partial u_j}\left[\left(\frac{\partial R_{1j}}{\partial x_1} - \frac{C_1}{2}\overline{\omega} u_j\right) f\right] + \frac{C_0}{2}\overline{\varepsilon}\frac{\partial^2 f}{\partial u_j u_j} \ , \tag{2.1}$$

where C_0 and C_1 are model constants, $R_{ij} = \overline{u_i u_j}$ is the Reynolds stress tensor, $\overline{k}$ is the mean turbulent kinetic energy, $\overline{\omega}$ is the mean dissipation frequency and $\overline{\varepsilon}$ is the mean dissipation rate. The Reynolds stress tensor R_{ij}

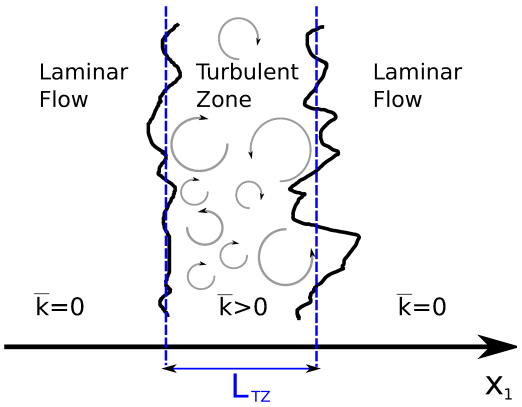

FIGURE 1. Sketch of a turbulent zone as studied in this work.

and $\overline{k}$ are obtained directly from the PDF by the relations :

$$\overline{k}(x_1,t) = \frac{1}{2}R_{ii}(x_1,t) = \frac{1}{2}\overline{u_i u_i}(x_1,t) \quad \text{and} \quad R_{ij}(x_1,t) = \overline{u_i u_j}(x_1,t) = \int_{\mathbb{R}^3} u_i u_j f(\mathbf{u};x_1,t)d\mathbf{u} \tag{2.2}$$

The dissipation rate and frequency are linked by the relation :

$$\overline{\omega}(x_1,t) = \frac{\overline{\varepsilon}(x_1,t)}{\overline{k}(x_1,t)} \tag{2.3}$$

An additional equation for the dissipation is required to close the system. As in standard $\overline{k}-\overline{\varepsilon}$ models, this equation is obtained by direct analogy with the equation of $\overline{k}$. The evolution of $\overline{k}$ deduced from the PDF equation (2.1) is :

$$\frac{\partial \overline{k}}{\partial t} + \frac{\partial}{\partial x_1}\left(\overline{u_1 k}\right) = -\overline{\varepsilon} \tag{2.4}$$

The evolution of $\overline{\varepsilon}$ is then set to :

$$\frac{\partial \overline{\varepsilon}}{\partial t} + \frac{\partial}{\partial x_1}\left(C_\varepsilon \overline{\omega}\ \overline{u_1 k}\right) = -C_{\varepsilon_2}\overline{\omega}\ \overline{\varepsilon} \tag{2.5}$$

where C_ε and C_{ε_2} are model constants and where $\overline{u_i k}$ is the following triple velocity correlation :

$$\overline{u_i k} = \frac{1}{2}\overline{u_i u_p u_p}$$

The values of the different constants appearing in the above equations are given in table 1. These values are taken from the litterature [1–4].

C_0	C_1	C_ε	C_{ε_2}
$\frac{2}{3}(C_1-1)$	1.5–5	1	1.9

TABLEAU 1. Model constants

Note that C_0 and C_1 are not independent : in order to ensure that $\overline{\varepsilon}$ is the dissipation rate of $\overline{k}$ one must have $C_0 = \frac{2}{3}(C_1 - 1)$. As noted in [2], the value of C_1 varies significantly in the litterature. It mostly depends on whether the SLM is used to model both the non-linear redistribution of energy and the rapid contribution of the pressure gradient, or whether it is associated with an additional component modelling the rapid pressure part. In the former case, the value of C_1 is usually set to higher values, typically $C_1 = 4.15$. In the latter case, it is set to lower values, typically $C_1 = 1.8$. In the absence of production, as in the TZ case considered here, there is no rapid pressure term and both low and high values of C_1 are acceptable.

3. Weakly inhomogeneous limit and diffusion regime

3.1. **Main assumption**

Two main lengths characterize the turbulent field in the TZ configuration, the integral length ℓ and the gradient length L. They are respectively defined as :

$$\ell = \frac{\overline{k}^{3/2}}{\overline{\varepsilon}} \quad \text{and} \quad L = \left[\frac{1}{\overline{k}}\frac{\partial \overline{k}}{\partial x_1}\right]^{-1}$$

The integral length ℓ is representative of the size of the turbulent eddies present in the turbulent zone, while L measures the inhomogeneity of the turbulent field and is expected to be roughly on the order of the turbulent zone size L_{TZ}.

We now make the assumption that the flow is weakly inhomogeneous, i.e. that turbulent eddies are much smaller than L. More precisely, we assume that :

$$\frac{\ell}{L} \sim \epsilon_a \ll 1 \tag{3.1}$$

Anticipating on a configuration where the PDF remains close to a Gaussian, this assumption can be incorporated in the equation (2.1) and (2.5) as :

$$\frac{\partial f}{\partial t} + \epsilon_a u_1 \frac{\partial f}{\partial x_1} = -\frac{\partial}{\partial u_j}\left[\left(\epsilon_a \frac{\partial R_{1j}}{\partial x_1} - \frac{C_1}{2}\overline{\omega} u_j\right) f\right] + \frac{C_0}{2}\overline{\varepsilon}\frac{\partial^2 f}{\partial u_j u_j} \tag{3.2}$$

$$\frac{\partial \overline{\varepsilon}}{\partial t} + \epsilon_a \frac{\partial}{\partial x_1}\left(C_\varepsilon \overline{\omega}\ \overline{u_1 k}\right) = -C_{\varepsilon_2}\overline{\omega}\ \overline{\varepsilon} \tag{3.3}$$

3.2. **Asymptotic expansion**

We look for a solution of equations (3.2) and (3.3) in the form of an expansion along the small parameter ϵ_a :

$$f = f^{(0)} + \epsilon_a f^{(1)} + \epsilon_a^2 f^{(2)} + \dots , \tag{3.4}$$

$$\overline{\varepsilon} = \overline{\varepsilon}^{(0)} + \epsilon_a \overline{\varepsilon}^{(1)} + \epsilon_a^2 \overline{\varepsilon}^{(2)} + \dots , \tag{3.5}$$

where we impose $\displaystyle\int_{\mathbb{R}^3} f^{(0)}(\mathbf{u}; x_1, t) d\mathbf{u} = 1$ and $\displaystyle\int_{\mathbb{R}^3} f^{(i)}(\mathbf{u}; x_1, t) d\mathbf{u} = 0, \forall i \geq 1$, without loss of generality.

The zeroth order of the expansion for f obeys a Fokker-Planck equation. Its asymptotic solution is an isotropic Gaussian of variance $\sigma^2 = \frac{2}{3}\overline{k}^{(0)}$. We will assume that the time is large enough so that this asymptotic solution is reached. Then, we have :

$$f^{(0)}(\mathbf{u}; x_1, t) = \frac{e^{-\frac{u_i u_i}{2\sigma^2}}}{(2\pi\sigma^2)^{3/2}} \quad \text{with} \quad \sigma^2 = \frac{2}{3}\overline{k}^{(0)}$$

where the zeroth order kinetic energy and its dissipation evolve according to :

$$\frac{\partial \overline{k}^{(0)}}{\partial t} = -\overline{\varepsilon}^{(0)} \quad , \quad \frac{\partial \overline{\varepsilon}^{(0)}}{\partial t} = -C_{\varepsilon_2} \frac{\overline{\varepsilon}^{(0)\,2}}{\overline{k}^{(0)}}$$

The variance $\overline{u_i u_j}^{(1)}$ and $\overline{\varepsilon}^{(1)}$ obey an autonomous system of equations. Zero being a particular solution of it, the choice we retain is

$$\overline{u_i u_j}^{(1)} = 0 \text{ and } \overline{\varepsilon}^{(1)} = 0$$

With this condition, we obtain :

$$f^{(1)} = C_g \frac{\sigma}{\omega} \frac{\partial_{x_1} \sigma^2}{\sigma^2} \;\; \frac{u_1}{\sigma} \left(5 - \frac{u_i u_i}{\sigma^2}\right) f^{(0)} \qquad \text{with } C_g = \frac{1}{3C_1 + 2C_{\varepsilon_2} - 6}$$

As explained above, $f^{(1)}$ does not contribute to the Reynolds stresses ($\overline{u_i u_j}^{(1)} = 0$). However, it yields the main contribution to the third order moments. From the previous formula, one has :

$$\overline{u_i u_j u_k}^{(1)} = -2C_g \frac{\sigma^2}{\omega} \frac{\partial \sigma^2}{\partial x_1} \left(\delta_{1i}\delta_{jk} + \delta_{1j}\delta_{ik} + \delta_{1k}\delta_{ij}\right) \tag{3.6}$$

In particular, the flux of kinetic energy is given by :

$$\overline{u_i k}^{(1)} = -5C_g \frac{\sigma^2}{\omega} \frac{\partial \sigma^2}{\partial x_1} \delta_{i_1} \tag{3.7}$$

The second order is not detailed here. It yields an anisotropic contribution to the Reynolds stresses and an even contribution to the PDF, with a dependency on the gradient of σ^2 and on its Laplacian.

3.3. **Main result : approximate PDF solution in the weakly inhomogeneous regime**

By collecting the main orders of the asymptotic expansion, we obtain that :

$$f(\mathbf{u}; x_1, t) = \left[1 + \sqrt{2/3} C_g \; \ell \frac{1}{\overline{k}} \frac{\partial \overline{k}}{\partial x_1} \; \frac{u_1}{2\overline{k}/3} \left(5 - \frac{u_i u_i}{2\overline{k}/3}\right)\right] \frac{e^{-u_i u_i / (4\overline{k}/3)}}{(4\pi \overline{k}/3)^{3/2}} \tag{3.8}$$

where $\overline{k}$ is solution of a $\overline{k} - \overline{\varepsilon}$-like system :

$$\frac{\partial \overline{k}}{\partial t} = \frac{\partial}{\partial x_1} \left(C_k \frac{\overline{k}^2}{\overline{\varepsilon}} \frac{\partial \overline{k}}{\partial x_1} \right) - \overline{\varepsilon} \tag{3.9}$$

$$\frac{\partial \overline{\varepsilon}}{\partial t} = \frac{\partial}{\partial x_1} \left(C_\varepsilon C_k \frac{\overline{k}^2}{\overline{\varepsilon}} \left(\frac{\partial \overline{\varepsilon}}{\partial x_1} - \overline{k} \frac{\partial \overline{\omega}}{\partial x_1} \right) \right) - C_{\varepsilon_2} \overline{\omega} \; \overline{\varepsilon} \tag{3.10}$$

with :

$$C_k = \frac{20}{9} C_g = \frac{20}{9\,(3C_1 + 2C_{\varepsilon_2} - 6)}$$

To obtain these expressions, we used the relations $\ell = \overline{k}^{3/2}/\overline{\varepsilon}$ and $\sigma^2 = 2\overline{k}/3$. We also injected relation (3.7) into the evolution equations (2.4)-(2.5) of $\overline{k}$ and $\overline{\varepsilon}$.

When $C_\varepsilon = 1$, as chosen in this study, the above $\overline{k} - \overline{\varepsilon}$ system admits an asymptotic self-similar solution, first found by Barenblatt & co-workers [9] and later by Cherfils & Harrison [10]. It is given by :

$$\overline{k}(x_1,t) = \overline{k}_0 \left(1 + {}^{t}/_{\tau_0}\right)^{-2+2\beta} \left(1 - \left[{}^{x_1}/_{\Lambda(t)}\right]^2\right) \quad , \quad \varepsilon(x_1,t) = \overline{\varepsilon}_0 \left(1 + {}^{t}/_{\tau_0}\right)^{-3+2\beta} \left(1 - \left[{}^{x_1}/_{\Lambda(t)}\right]^2\right) \ , \tag{3.11}$$

$$\text{with } \Lambda(t) = \Lambda_0 \left(1 + {}^{t}/_{\tau_0}\right)^{\beta} \quad \text{and} \quad \beta = \frac{2C_{\varepsilon_2} - 3}{3(C_{\varepsilon_2} - 1)} \tag{3.12}$$

The values of $\overline{k}$ and $\overline{\varepsilon}$ at $t = 0$ and $x_1 = 0$ are related to the two free parameters defining the initial length of the profile Λ_0 and the initial turbulent time τ_0 :

$$\tau_0 = \frac{1}{C_{\varepsilon_2} - 1} \frac{\overline{k}_0}{\overline{\varepsilon}_0} \quad , \quad \Lambda_0 = \sqrt{\frac{2C_k}{\beta(C_{\varepsilon_2} - 1)}} \frac{\overline{k}_0^{3/2}}{\overline{\varepsilon}_0} \tag{3.13}$$

Equations (3.8)-(3.10), with their analytic solution (3.11)-(3.13), are the main result of this work. They show that, in the weakly inhomogeneous regime, the simplified Langevin PDF model behaves as a standard $\overline{k} - \overline{\varepsilon}$ model. In particular, turbulent transport is given on first order by a diffusion term which coefficient depends explicitely on two model constants : C_1 and C_{ε_2}. The physical implications of this finding will be discussed in section 5.

4. Numerical validation

In order to gain confidence in the solution derived in section 3.2, we would like to provide, *a posteriori*, the numerical evidence that the derived PDF shapes (3.8) are observed and correspond to the diffusion regime described by equations (3.9)-(3.10). To do so, we use two different numerical solvers.

- The first one is a Eulerian Monte Carlo (EMC) solver and is applied to solve equations (2.1) and (2.5). EMC methods have been introduced in [11, 12] and have been extended to include the velocity field in [13].
- The second one is a direct deterministic solver based on finite volume approximations and described in appendix A. Given the high number of dimensions of equation (2.1), the computational cost of a deterministic method is too expensive. Hence, we decide to apply the deterministic method to a simplified version of equations (2.1) and (2.5). This simplified system is described in section 4.2.

4.1. **Eulerian Monte Carlo simulations**

First, we solve equations (2.1) and (2.5) with a Eulerian Monte Carlo (EMC) solver. The parameters of the simulation are the following. The computational domain $[x_{min}, x_{max}]$ is set to $[-80, 80]$. It is discretized with $N_x = 256$ points. The number of stochastic fields is set to $N_f = 16000$. The initial conditions are set according to the expected solution (3.11) :

$$\overline{k}(x_1, t=0) = \overline{k}_0 \left(1 - \left[\frac{x_1}{\Lambda_0}\right]^2\right) \quad , \quad \varepsilon(x_1, t=0) = \overline{\varepsilon}_0 \left(1 - \left[\frac{x_1}{\Lambda_0}\right]^2\right)$$

where we set the values $\Lambda_0 = 10$ and $\overline{k}_0 = 1.5$ and where the values of τ_0 and $\overline{\varepsilon}_0$ are given by formula (3.13). Two calculations are done : one with $C_1 = 4.15$ and one with $C_1 = 1.8$. For $C_1 = 1.8$, one has $\tau_0 = 2.0$ and $\overline{\varepsilon}_0 = 0.84$ and for $C_1 = 4.15$, one has $\tau_0 = 3.6$ and $\overline{\varepsilon}_0 = 0.47$.

4.1.1. *Self-similarity*

In order to assess the self-similarity of the solution, we focus on the following three parameters :

$$\overline{k}_{max}(t) = \max_{x_1 \in \mathbb{R}} \left(\overline{k}(x_1,t)\right) \quad , \quad \overline{\varepsilon}_{max}(t) = \max_{x_1 \in \mathbb{R}} \left(\overline{\varepsilon}(x_1,t)\right) \quad \text{and} \quad L_k = \frac{3}{4} \frac{\int \overline{k}(x_1,t) dx_1}{k_{max}}$$

The ratio $\overline{k}/k_{max}$ taken at different times is displayed on figure 2 as a function of x_1/L_k and for two values of C_1. It can be seen that the respective profiles of the two ratios fall approximately on a single curve. This indicates that $\overline{k}$ is close to a self-similar state. Besides, the collapsed curves remain close to parabolas as predicted by solution (3.9)-(3.10). The main difference with this solution occurs at the edges of the turbulent zone : while equations (3.9)-(3.10) predict a compact support for $\overline{k}$, the simulation yields a non-compact one. While not displayed here, the same conclusions also apply to $\overline{\varepsilon}$.

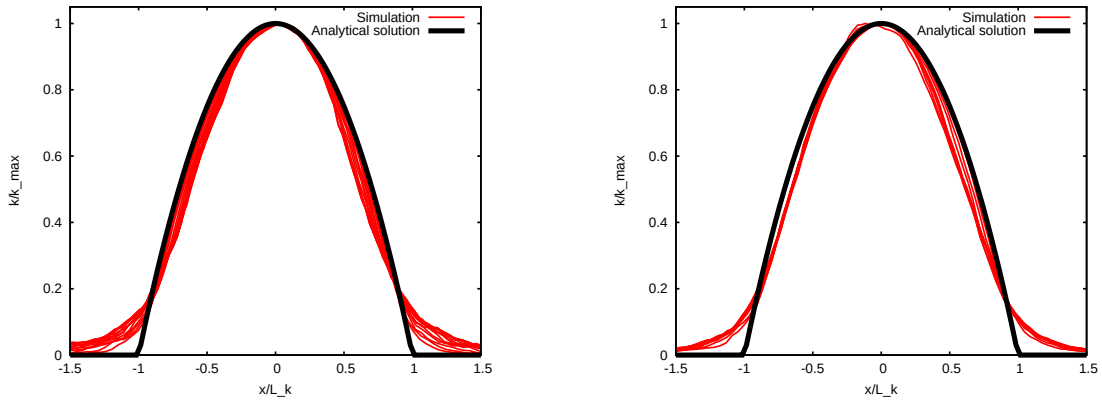

(a) $C_1 = 1.8$ (b) $C_1 = 4.15$

FIGURE 2. $\overline{k}/\overline{k}_{max}$ as a function of x_1/L_k at different times from $t/t_0 = 0.3$ to $t/t_0 = 5$

We now consider the time evolutions of the three parameters $\overline{k}_{max}$, $\overline{\varepsilon}_{max}$ and L_k and compare them against their predicted values given by the self-similar solution (3.9)-(3.10). To this end, we introduce the three ratios R_k, R_ε and R_L defined by :

$$R_k = \frac{\overline{k}_{max}}{\overline{k}_0 \left(1 + t/\tau_0\right)^{-2+2\beta}} \quad , \quad R_\varepsilon = \frac{\overline{\varepsilon}_{max}}{\overline{\varepsilon}_0 \left(1 + t/\tau_0\right)^{-3+2\beta}} \quad , \quad R_L = \frac{L_k}{\Lambda_0 \left(1 + t/\tau_0\right)^{\beta}}$$

If the self-similar solution (3.9)-(3.10) applies, then R_k, R_ε and R_L should become independent of time. Besides, given that the initial condition was chosen close to a self-similar solution, one should have $R_k = R_\varepsilon = R_L \approx 1$. A strict equality is not expected since the initial is not fully coherent with the self-similar state. In particular, the initial PDF is a Gaussian, whereas the self-similar PDF deviates from Gaussianity.

The three ratios R_k, R_ε and R_L are displayed in figure 3. It can be seen that they indeed remain approximately constant and stay close to one for the two simulations respectively performed with $C_1 = 1.8$ and $C_1 = 4.15$. As a conclusion, the self-similar solution (3.9)-(3.10) appears to be in good agreement with the simulation results.

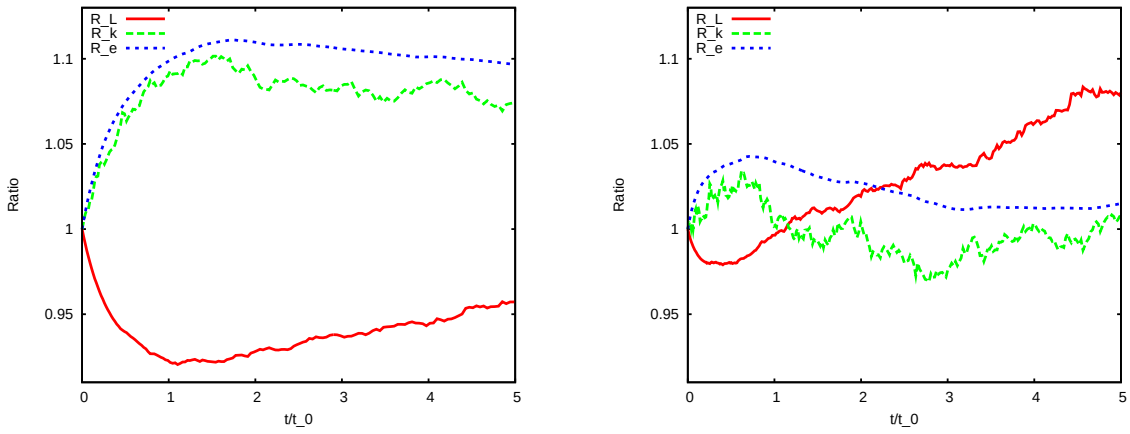

(a) $C_1 = 1.8$ (b) $C_1 = 4.15$

FIGURE 3. Evolution of R_k, R_ε and R_L as a function of time.

4.1.2. *Flux of kinetic energy*

The existence and properties of the self-similar solution arise from the approximation of the flux of kinetic energy given by formula (3.7). To check this approximation, we introduce the non-dimensional flux :

$$F^*(x_1,t) = \frac{\overline{u_1 k}}{\overline{k}_{max}^{3/2}\sqrt{2\beta C_k(C_{\varepsilon_2}-1)}}$$

According to formula (3.7), F^* should be equal to $x_1/L_k(1-[x_1/L_k]^2)$. The comparison between the two functions is displayed in figure 4 at different times. It can be seen that both simulation and prediction are in good agreement in the central part of the mixing zone, from $x_1/L_k \in [-0.7, 0.7]$. Outside, the gradient diffusion assumption ceases to be relevent : the predicted flux of kinetic energy becomes much smaller than the simulated flux. This observation is consistent with the one made on the non-compactness of the $\overline{k}-\overline{\varepsilon}$ profiles observed in figure 2.

4.2. **Deterministic finite volume simulations**

The Eulerian Monte Carlo method has allowed to study some properties of the second and third order moments of the velocity field. However, its intrisic noise is too high to directly study the PDF. To circumvent this deficiency, we propose to use a deterministic solver.

4.2.1. *Simplification of system* (2.1)-(2.5)

As explained above, equations (2.1)-(2.5) have a high number of dimenions : 1 in time and 4 in velocity and physical space. The computational cost of a deterministic method is too expensive so that we propose to simplify these equations in order to reduce their dimensionality. More precisely, we focus on the the marginal PDF f_1 of u_1. By integrating equation (2.1) over u_2 and u_3, one obtains that f_1 evolves as :

$$\frac{\partial f_1}{\partial t} + u_1\frac{\partial f_1}{\partial x_1} = -\frac{\partial}{\partial u_1}\left[\left(\frac{\partial \overline{u_1^2}}{\partial x_1} - \frac{C_1}{2}\overline{\omega}u_1\right)f_1\right] + \frac{C_1-1}{2}\overline{\varepsilon}^*\frac{\partial^2 f_1}{\partial u_1 u_1}\ , \tag{4.1}$$

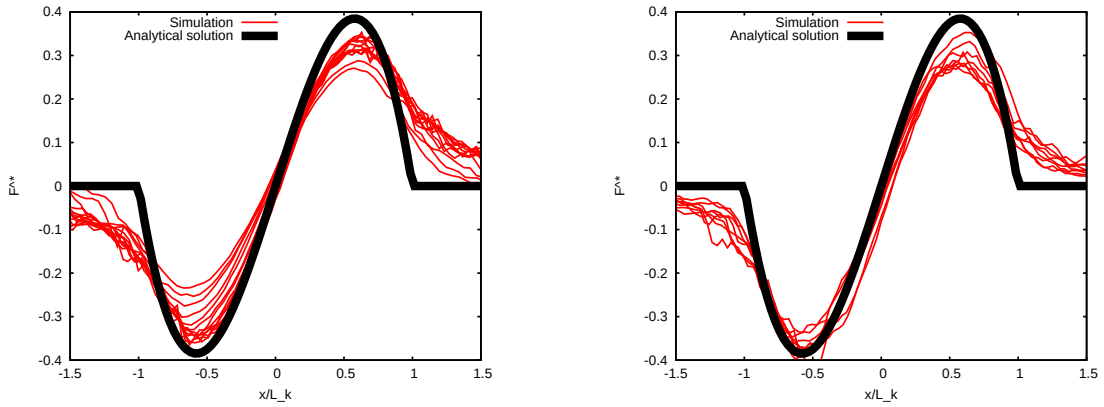

(a) $C_1 = 1.8$ (b) $C_1 = 4.15$

FIGURE 4. F^* as a function of x_1/L_k at different times from $t/t_0 = 1$ to $t/t_0 = 5$.

where $\overline{\varepsilon}^* = \frac{2}{3}\overline{\varepsilon}$ is the dissipation of $\overline{u_1^2}$. This equation is closed provided the evolution of $\overline{\varepsilon}^*$ is known in terms of the statistics of u_1. This is not the case of equation (2.5) which is related to $\overline{k}$. Hence, we propose to simplify this equation. Namely, we assume that the Reynolds stresses are strictly isotropic. Then, the turbulent frequency can be related to $\overline{u_1^2}$ according to : $\omega = \overline{\varepsilon}/\overline{k} = \overline{\varepsilon}^*/\overline{u_1^2}$. Besides, we assume that $\overline{u_1 u_i u_j}$ is also an isotropic tensor, which yields $\overline{u_1 k} = 3\overline{u_1^3}/2$. With these assumptions, one deduces from equation (2.5) the following simplified evolution for $\overline{\varepsilon}^*$:

$$\frac{\partial \overline{\varepsilon}^*}{\partial t} + \frac{\partial}{\partial x_1}\left(C_\varepsilon \overline{\omega}\ \overline{u_1^3}\right) = -C_{\varepsilon_2}\overline{\omega}\ \overline{\varepsilon}^* \tag{4.2}$$

Equations (4.1)-(4.2) are three dimensional and can be solved with the deterministic solver. They share the same properties as equations (2.1)-(2.5) but present a slight variation in the weakly inhomogeneous limit. The limit of f_1 is, as expected, the integral of the limit of f (3.8) over u_2 and u_3 :

$$f_1(u_1; x_1, t) = \frac{e^{-u_1^2/(2\overline{u_1^2})}}{\sqrt{2\pi\overline{u_1^2}}}\left(1 + C_g\left(\frac{1}{\sqrt{\overline{u_1^2}}\omega}\frac{\partial \overline{u_1^2}}{\partial x_1}\right)\frac{u_1}{\sqrt{\overline{u_1^2}}}\left(3 - \frac{u_1^2}{\overline{u_1^2}}\right)\right)\ , \tag{4.3}$$

However, the value of $\overline{u_1^3}$ is not given by formula (3.6) but by :

$$\overline{u_1^3} = -C_k \frac{\overline{u_1^2}}{\omega}\frac{\partial \overline{u_1^2}}{\partial x_1}$$

with $C_k = 6C_g$. The notation C_k has been retained here because in the diffusion limit, $\overline{u_1^2}$ and $\overline{\varepsilon}^*$ obey a $\overline{k} - \overline{\varepsilon}$ like system similar to equations (3.9)-(3.10). The solution of this system is then obtained directly from equations (3.11) by replacing $\overline{k}$ by $\overline{u_1^2}$ and $\overline{\varepsilon}$ by $\overline{\varepsilon}^*$.

4.2.2. *Set-up*

The computational domain is defined by $[x_{min}, x_{max}] = [-30, 30]$ and $[u_{min}, u_{max}] = [-6, 6]$. It is discretized with $(n_x, n_{vx}) = 256^2$ points and the time step is set to $dt = 2 \cdot 10^{-3}$. The initial conditions are set according to

$$\overline{u_1^2}(x_1, t = 0) = \overline{k}_0 \left(1 - \left[\frac{x_1}{\Lambda_0}\right]^2\right) + \overline{k}_{min} \quad , \quad \varepsilon^*(x_1, t = 0) = \overline{\varepsilon}_0 \left(1 - \left[\frac{x_1}{\Lambda_0}\right]^2\right)$$

where $\overline{k}_0 = 1$ and $\Lambda_0 = 10$ and where the values of τ_0 and $\overline{\varepsilon}_0$ are given by formula (3.13). The additional parameter $\overline{k}_{min}$ is set to $\overline{k}_{min} = 10^{-2}$. It is required because Diracs cannot be represented in a deterministic method. They are here replaced by a Gaussian with a variance sufficiently small for the PDF to approximate a Dirac, and sufficiently large to obtain a numerical resolution of the PDF with a reasonable number of velocity points.

The coefficients of the model are set such as $C_1 = 2.73$, in order to recover $C_k = 1$.

4.2.3. *Comparison with analytical PDF solutions*

For the TMZ configuration described in section 4.2, we first compare the diffusion solution (3.11), and the numerical solution of the equations (4.1)-(4.2). In the figures 5 and 6, we observe a good agreement between the numerical and the analytical solutions, for the second and third moments of the PDF. Moreover, in figure 7, the self-similality of the solution is checked, with respect to the quantities R_k, R_ϵ and R_L (that are defined in section 4.1.1). This shows that the PDF solution operates close to the diffusion regime, for which asymptotic PDF solutions have been derived in section 3.2.

Then, we can legitimately analyse the anisotropic, odd part of the PDF, with respect to the analytical one (denoted as $\epsilon_a f^1$ in section 3.2). The comparison between the numerical and analytical PDF is shown in figure 8, respectively at the center and at the edge of the TMZ. At the end of the simulation, the anisotropy of the PDF is greater at the edge than at the center of the TMZ. This can be seen *via* the value of the small expansion parameter, which stabilizes at $\epsilon_a = 5.10^{-3}$ at the center of the TMZ, and $\epsilon_a = 0.8$ at the edge of the TMZ. The validity range of the expansion is therefore not verified *a posteriori* at all points of the domain. However the PDF shapes are qualitatively the same, and the TMZ diffuses at the correct rate. This gives confidence in the asymptotic expansion derived in section 3.2.

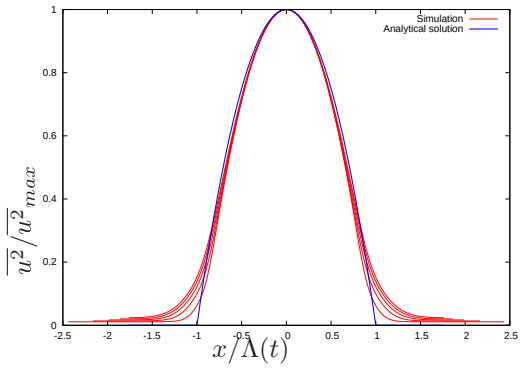

FIGURE 5. Turbulent kinetic energy from $t/t_0 = 1$ to $t/t_0 = 5$. Comparison between Barenblatt analytical solution [9] and the numerical PDF solution.

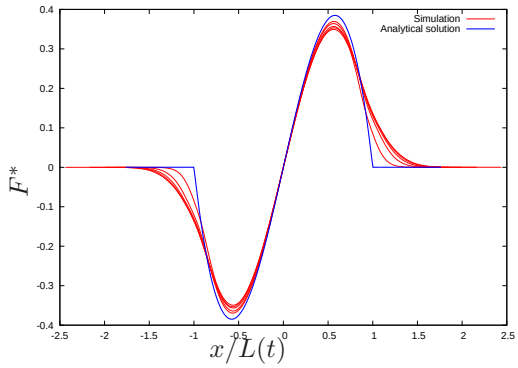

FIGURE 6. Normalized third order moment from $t/t_0 = 1$ to $t/t_0 = 5$. Comparison between Barenblatt analytical solution [9] and the numerical PDF solution.

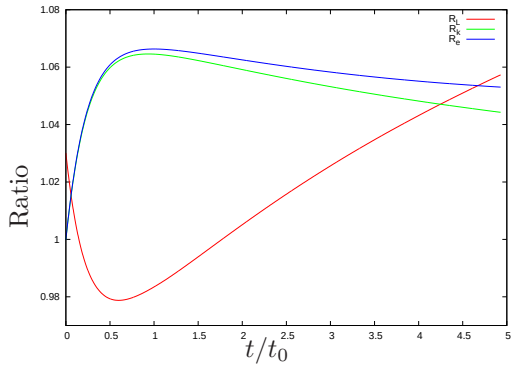

FIGURE 7. Evolution of R_k, R_ϵ, and R_L as a function of time.

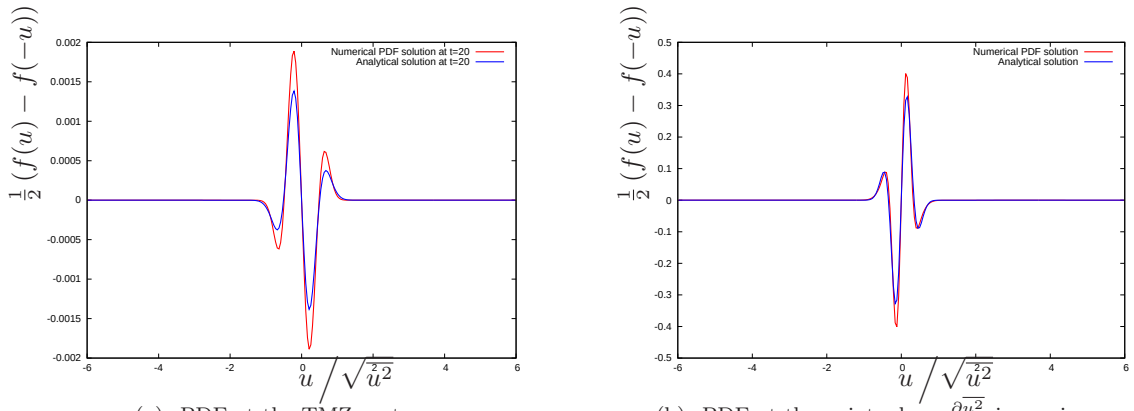

(a) PDF at the TMZ center

(b) PDF at the point where $\frac{\partial \overline{u^2}}{\partial x}$ is maximum

FIGURE 8. Even part of the PDF. Comparison bewteen the numerical PDF and the solution obtained from the asymptotic development, at $t/t_0 = 5$.

5. DISCUSSION AND CONCLUSIONS

In section 3, we showed that, in the weakly inhomogeneous limit, the simplified Langevin PDF model gives rise to diffusion approximation for turbulent transport and behaves as a standard $\overline{k} - \overline{\varepsilon}$ model. In section 4,

we performed numerical simulations of a turbulent mixing zone and showed that the weakly inhomogeneous limit and the diffusion approximation were relevent to describe the diffusion and decay of turbulence in this configuration.

These results raise a number of questions concerning the way turbulent transport is effectively modelled in Langevin PDF models. First, the transport of kinetic energy is given on first order by a gradient diffusion approximation. The corresponding diffusion coefficient C_k is found to depend explicitely on two model constants : C_1 and C_{ε_2}. We recall that the constant C_{ε_2} is set in order to reproduce the correct decay of kinetic energy in homogeneous isotropic turbulence. As for the constant C_1, it is set in order to specify the decay of the anisotropy tensor $b_{ij} = R_{ij} - 2\overline{k}/3\delta_{ij}$ in homogeneous turbulence. Hence, one is faced with an apparent contradiction : the coefficient controlling turbulent transport in Langevin PDF methods is set by observations and reasonings made in homogeneous turbulence, which by definition is devoid of turbulent transport.

Second, the value of C_1 varies in the litterature and so does the value of the diffusion coefficient C_k. For $C_1 = 1.8$, one has $C_k = 0.7$ and for $C_1 = 4.15$, one has $C_k = 0.22$. These values have to be compared with the usual value retained in $\overline{k} - \overline{\varepsilon}$ models $C_k^{\overline{k}-\overline{\varepsilon}} = 0.15 - 0.22$. Thus, if one wants to obtain results close to a standard $\overline{k}-\overline{\varepsilon}$ model in the diffusion-dissipation regime, one should rather choose a value of $C_1 = 4.15$. However, as explained in section 2, higher values of C_1 are usually associated with simpler models discarding the rapid contribution of the pressure gradient. For more realistic models, it is the value $C_1 = 1.8$ which is relevant. Hence, one is left to choose between a value of C_1 that captures correctly turbulent transport and a value that is compatible with the presence of a rapid pressure model. In addition to the first comment, this second remark tends to indicate that the definition of C_1 and the term it controls in the simplified Langevin model is overloaded. It looks as if the C_1 term in equation (2.1) had to represent two distinct physical mechanisms : return to isotropy and turbulent transport.

Finally, a last remark must be made. While the Langevin PDF and $\overline{k}-\overline{\varepsilon}$ models behave alike in the diffusion limit, there is still a fundamental difference between the two. In the $\overline{k} - \overline{\varepsilon}$ model, the gradient diffusion term models turbulent advection and also turbulent transport by the pressure : $-C_k^{\overline{k}-\varepsilon}\frac{\overline{k}^2}{\overline{\varepsilon}}\partial_{x_i}\overline{k} = \overline{u_i k} + \overline{u_i p}$. By contrast, in the simplified Langevin PDF model, pressure transport is neglected. This can be seen in equation (2.4) where only the flux of $\overline{k}$ appears. For the simplified Langevin model, one has : $-C_k\frac{\overline{k}^2}{\overline{\varepsilon}}\partial_{x_i}\overline{k} = \overline{u_i k}$. This relation could be justified if $\overline{u_i p}$ was negligible. However, this is not the case. In isotropic turbulence, one has exactly : $\overline{u_i p} = -2/5\overline{u_i k}$ [14]. Therefore, an important part of turbulent transport is missing in PDF models. Still, the fact that $\overline{u_i p}$ and $\overline{u_i k}$ are proportional allows for an effective definition of C_k which accounts for the missing term and give an overall correct transport in the diffusion regime. In that case, the value of $\overline{u_i k}$ is overestimated by a factor $5/3 \approx 1.7$.

All these remarks point to some deficiencies in the way turbulent transport is represented in PDF models. We hope to adress some of these deficiencies in a forthcoming paper.

A. Deterministic direct method

We propose here a Finite Volume numerical method to discretize the equation (4.1), where the space, velocity fluctuation and time dimensions are discretized to yield a unique value of the PDF $f_1(u_1; x_1, t)$. This numerical scheme should allow to statisfy the following constraints :

$$f_1(u_1; x_1, t) \geq 0 \,, \tag{A.1}$$

$$\int_{\mathbb{R}} f_1(u_1; x_1, t) du_1 = 1 \,, \tag{A.2}$$

$$\int_{\mathbb{R}} u_1 f_1(u_1; x_1, t) du_1 = 0 \,. \tag{A.3}$$

To simplify notations, we will hereafter drop the index 1 from x_1 and f_1.

We introduce a cartesian, uniform mesh, defined by the control volumes $\mathcal{C}_{i,j} = \left[x_{i-1/2}, x_{i+1/2}\right] \left[u_{j-1/2}, u_{j+1/2}\right]$, where $(i,j) \in I \times J \subset \mathbb{N} \times \mathbb{Z}$. We define Δx and Δv as the sizes of the space and velocity control volumes, respectively. $x_i = i\Delta x$ and $u_j = j\Delta v$ here refer to the cell centers, whereas $x_{i+1/2} = (i+1/2)\Delta x$ and $u_{j+1/2} = (j+1/2)\Delta u$ refer to the volume control boundaries.
Let $f_{i,j}^n$ be an average approximation of the PDF on the control volume at time $t^n = n\Delta t$, $n \in \mathbb{N}$,

$$f_{i,j}^n = \frac{1}{\Delta x \Delta v} \int_{\mathcal{C}_{i,j}} f(x,u,t^n) du dx \ . \tag{A.4}$$

We start from the Finite Volume scheme originally derived in [15]. We recall the basic steps leading to its construction on the simplified advection equation

$$\frac{\partial f}{\partial t} + u \frac{\partial f}{\partial x} = 0 \ , u > 0 \ , \tag{A.5}$$

for the sake of simplicity. Its extension by symmetry to the negative velocity space is straighforward. Its application to the right-hand side, velocity drift terms, in equation (4.1), will be discussed herebelow.
First, a time explicit Euler scheme is employed to discretize the equation (A.5) as

$$f_i^{n+1} = f_i^n + u \frac{\Delta t}{\Delta x} \left(F_{i+1/2}^n - F_{i-1/2}^n \right) \ , \tag{A.6}$$

where $F_{i+1/2}^n = F(x_{i+1/2}, t^n)$ stands as a discrete conservative approximation of $f(x,t)$ on the boundary of the control volume $\left[x_{i-1/2}, x_{i+1/2}\right]$. Second, following [15], a second order MUSCL reconstruction technique (by primitive), leads to the approximation

$$F(x,t^n) = \left[f_i^n + \epsilon^+ \frac{x - x_i}{\Delta x} \left(f_{i+1}^n - f_i^n \right) \right] \ , \ \forall x \in \left[x_{i-1/2}, x_{i+1/2}\right] \ . \tag{A.7}$$

The slope limiter ϵ^+ is introduced in order to recover the maximum priciple $0 \leq f_i^n \leq \|f\|_\infty$ under the CFL condition $u\frac{\Delta t}{\Delta x} \leq 1$. Its expression, given by

$$\epsilon^+ = \begin{cases} 0 \ , \text{if } \left(f_{i+1}^n - f_i^n \right) \left(f_i^n - f_{i-1}^n \right) < 0 \\ \min\left(1, \dfrac{2\left(\|f\|_\infty - f_i^n \right)}{f_i^n - f_{i+1}^n} \right) \ , \text{if } \left(f_{i+1}^n - f_i^n \right) < 0 \\ \min\left(1, \dfrac{2 f_i^n}{f_{i+1}^n - f_i^n} \right) \ , \text{else} \end{cases} \tag{A.8}$$

leads to a nonlinear expression for the numerical flux.

This approximation procedure can be further extended to evaluate the velocity drift term in the right hand side of equation (4.1), which involves the velocity variance gradient $\dfrac{\partial \overline{u^2}}{\partial x}$. This drift term should balance with the advection term in the left hand side of equation (4.1), in order to guarantee the zero mean velocity conservation (A.3). At the discrete level, this requirement is met with a re-definition of $\left.\dfrac{\partial \overline{u^2}}{\partial x}\right|_i^n$ as a function of the discrete, reconstructed, numerical flux obtained for the advection term (left hand side of equation (4.1))

$$\left.\frac{\partial \overline{u^2}}{\partial x}\right|_i^n = \sum_j u_j^2 \frac{F_{i+1/2,j}^n - F_{i-1/2,j}^n}{\Delta x} \Delta v \Bigg/ \left(- \sum_j u_j \frac{F_{i,j+1/2}^n - F_{i,j-1/2}^n}{\Delta v} \Delta v \right) \ , \tag{A.9}$$

which is the analogous of the continuous relation, obtained by integration by parts,

$$\frac{\partial \overline{u^2}}{\partial x} = \int_{\mathbb{R}} du u^2 \frac{\partial f}{\partial x} \Big/ \left(- \int_{\mathbb{R}} du u \frac{\partial f}{\partial u} \right) . \tag{A.10}$$

The chosen discrete definition (A.9) mimics the integration by part (A.10) required to satisty the zero mean velocity conservation (A.3), that is $\overline{u} = 0$.
A similar procedure is now applied to the C_1 term in the right hand side of equation (4.1), which is rewritten as

$$\frac{\partial}{\partial u} \left(\frac{C_1}{2} \omega u f \right) \to \frac{\partial}{\partial u} \left(\frac{C_1}{2} \omega \left(u - \overline{u} \right) f \right) . \tag{A.11}$$

An extension of the Finite Volume scheme (A.6)-(A.7)-(A.8) is employed here, to the more general case where the fluxes depend on the drift variable u. This dependance is treated with a conservative centered discretization of the velocity variable in the flux uf. A discrete definition for $\overline{u}$ is required at this point in (A.11). We introduce an approximation that satisfies the zero mean velocity conservation in a discrete manner on the discrete analogous of the equation (A.11)

$$\overline{u}_i^n = \sum_j u_j \frac{F^n_{i,j+1/2} - F^n_{i,j-1/2}}{\Delta v} \Delta v \Big/ \left(\sum_j u_j \frac{u_{j+1/2} F^n_{i,j+1/2} - u_{j-1/2} F^n_{i,j-1/2}}{\Delta v} \Delta v \right) , \tag{A.12}$$

which is the discrete analoguous of the continuous expression

$$\overline{u} = \int_{\mathbb{R}} du u \frac{\partial f}{\partial u} \Big/ \int_{\mathbb{R}} du \frac{\partial}{\partial u} \left(uf \right) = 0 . \tag{A.13}$$

We finally obtain un unsplit discretization for all the advection terms in equation (4.1). The discrete analogous of the probability density conservation (A.2) is satisfied if the slope limiters are not active for the advection term $u \dfrac{\partial f}{\partial x}$. In this case, we indeed obtain a centered discretization whatever the sign of the velocity is. We accept a small deviation from the probability density conservation, where the limiters are active to guarantee the maximum principle.

We now turn to the discretization of the C_0 operator in the right hand side of equation (4.1). This term is splitted and discretized with an centered, implicit scheme, with net flux boundary conditions on the velocity space. This ensures the respect of the conservations (A.2) and (A.3), at the discrete level. Moreover, we obtain a M-matrix with a positive right hand side, leading to a positive PDF.
Finally, we remark that the splitting of the C_0 operator is convenient in the sense that it allows both the implicitation of this term and an easy implementation of a parallelisation on the space dimension x with good expected scalability. We have made use of the MPI parallelisation protocol to do so.

Références

[1] S. B. Pope. PDF methods for turbulent reactive flows. *Prog. Energ. Combust.*, 27 :119–192, 1985.

[2] S.B. Pope. On the relationship between stochastic Lagrangian models of turbulence and second-moment closures. *Phys. Fluids*, 6 :973–985, 1994.

[3] S. B. Pope. *Turbulent flows*. Cambridge Univ. Press, 2000.

[4] R. O. Fox and P. K. Yeung. Improved lagrangian mixing models for passive scalars in isotropic turbulence. *Phys. Fluids*, 15(4) :961–985, 2003.

[5] B.A. Younis, T.B. Gatski, and C.G. Speziale. Towards a rational model for the triple velocity correlations of turbulence. Technical Report TM-1999-209134, NASA, April 1999.

[6] I. Vallet. Reynolds stress modeling of three-dimensional secondary flows with emphasis on turbulent diffusion closure. *J. App. Mech.*, 74 :1142–1155, November 2007.

[7] P.R. Van Slooten, Jayesh, and S.B. Pope. Advances in PDF modeling for inhomogeneous turbulent flows. *Phys. Fluids*, 10(1) :246–265, 1998.
[8] K. Hanjalic and B.E. Launder. A Reynolds stress model of turbulence and its application to thin shear flows. *J. Fluid Mech.*, 52 :609–638, 1972.
[9] G.I. Barenblatt. Self-similar turbulence propagation from an instantaneous plane source,. *Nonlinear Dynamics and Turbulence*, pages 48–60, 1983.
[10] C. Cherfils and A.K. Harrison. Comparison of different statistical models of turbulence by similarity methods. In *Proceedings of the Fluids Engineering Division Summer Meeting*, Incline Village, Nevada, USA, June 1994. ASME.
[11] L. Valiño. A field Monte Carlo formulation for calculating the probability density function of a single scalar in a turbulent flow. *Flow, turbulence and combustion*, 60 :157–172, 1998.
[12] V. A. Sabel'nikov and O. Soulard. Rapidly decorrelating velocity field model as a tool for solving Fokker-Planck PDF equations of turbulent reactive scalars. *Phys. Rev. E*, 72 :016301, 2005.
[13] O. Soulard and V. A. Sabel'nikov. Eulerian Monte Carlo method for the joint velocity and mass-fraction probability density function in turbulent reactive gas flow combustion. *Explosion and Shock Waves*, 42(6) :753–762, 2006.
[14] J.L. Lumley. Computational modeling of turbulent flows. *Adv. Appl. Mech.*, 18 :123–176, 1978.
[15] F. Filbet, E. Sonnendrücker, and P. Bertrand. Conservative numerical schemes for the Vlasov equation. *J. Comp. Phys.*, 172(1) :166–187, 2001.